Modified Discrete Radon Transforms and Their Application to Rotation-Invariant Image Analysis

Mahmoud R. Hejazi, Georgy Shevlyakov, Yo-Sung Ho
Department of Information & Communications,
Gwangju Institute of science and Technology (GIST)
Gwangju, South Korea
{m_hejazi,shev,hoyo}@gist.ac.kr

Abstract—**This paper presents two novel transforms based on the discrete Radon transform. The proposed transforms smartly solve two inherent problems of the Radon transform in rotation estimation in digital images, i.e., direction-dependency and nonhomogeneity, that come from the different numbers of pixels projected on a line for different directions and/or coordinates of a direction. While the first transform considers the sample mean operator on the same sets of pixels for a direction instead of summation in the discrete Radon transform, the second transform uses the mean operator on sets of pixels with the equal number of elements. In order to show the efficiency of the proposed transforms, we apply them on image collections from the Brodatz album for estimating the directional information. Experimental results show a significant increase in correct estimation as well as in the processing time compared to the conventional Radon transform.**

Keywords—Radon transform, rotation-invariancy, texture analysis, direction estimation;

Topic area—Multimedia Databases (Content Analsysis).

I. INTRODUCTION

The Radon transform has received much attention in recent years. The capability of the Radon transform in transforming lines (line-trends) inside an image into a domain of possible line parameters even for a very noisy image has led to many line detection applications within image processing, computer vision, seismology, etc. The inverse Radon transform has also shown its worth in different fields such as electron microscopy, geophysical exploration, and imaging by ultrasound, X-ray, and magnetic resonance [1],[2].

Although the Radon transform is not by itself a tool for rotation estimation in an image, it may be used by some other tools to capture the directional information of an image which is necessary for rotation-invariant image analysis [3],[4]. Specifically, if we define the principle direction for an image as the direction along which the image has more straight lines, the Radon transform along this direction is usually expected to have larger variations [5], especially if we filter out the low frequency information from the image before applying the Radon transform [6].

However, for extracting the directional information, the Radon transform suffers from two inherent problems which have not been yet, to the best of our knowledge, tackled systematically. Let us consider the discrete Radon transform in order to clarify these problems. A similar idea can be depicted for the continuous case as well. In general, the Radon transform represents an image as a collection of projections along various line directions and corresponding coordinates along the directions. As a result, the number of pixels projected on a line is not the same for different directions and/or coordinates of a direction.

While the different number of pixels on a line in different directions makes the method direction-dependent (anisotropic), the different number of pixels in different coordinates of a direction may result to a nonhomogeneous analysis. There are some simple techniques that may handle the problems to some extent, e.g. taking the Radon transform on a disk shape area from the middle of the image instead of the whole image to make the method isotropic. However, since these solutions do not concentrate on the inherent source of problems directly, they may neither be always applicable nor increase the performance considerably, in many applications.

In the paper, we propose two different transforms based on the definition of the discrete Radon transform, where the first transform has a linear, and the second one has a nonlinear relation with the Radon transform. We will see that the proposed transforms not only solve the mentioned problems, but preserve the applicability of the Radon transform, as well.

In order to show the efficiency of these transforms in the rotation-invariant image analysis, we utilize them for the purpose of direction estimation and examine their performance on standard texture images from the Brodatz album [7]. Through different experiments, we evaluate their performance and compare it to the Radon transform. Robustness of the methods to the additive noise and their processing times are also examined. Experimental results show that the proposed transforms significantly outperform the conventional Radon transform.

II. BACKGROUND

The Radon transform is the projection of the image intensity along a radial line oriented at a specific angle. It transforms a 2-D image with lines (line-trends) into a domain of the possible line parameters ρ and θ, where ρ is the smallest distance from the origin and θ is its angle with the x-axis. In this form, a line is defined as

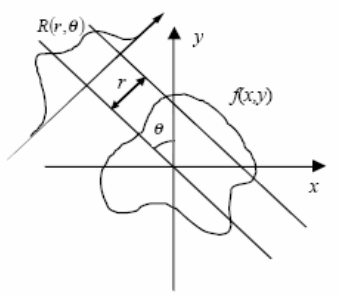

Figure 1. Radon transform of a typical 2-D image $f(x,y)$.

$$\rho = x\cos\theta + y\sin\theta). \tag{1}$$

Considering this definition of a line, the Radon transform of a 2-D image $f(x,y)$ can be then defined as

$$R(\rho,\theta) = \int_{-\infty}^{+\infty}\int_{-\infty}^{+\infty} f(x,y)\delta(\rho - x\cos\theta - y\sin\theta)dxdy. \tag{2}$$

Fig. 1 exhibits the Radon transform of a typical image for a reference line with parameters ρ and θ. However, for applying the Radon transform on a 2-D digital image, we first need to discretize the continuous equation. In practice, there are some different ways to approximate the discrete form [2]. Here, we solve this problem in a slightly different way which is more convenient for our goal in this paper. For this purpose, we use an equivalent form of (2), defined as

$$R(\rho,\theta) = \int_{-\infty}^{+\infty} f(\rho\cos\theta - s\sin\theta, \rho\sin\theta + s\cos\theta)ds, \tag{3}$$

where the s-axis lies along the line. Note that in (3), ρ and s can be calculated from x, y, and θ using (1) and the following equation, respectively:

$$s = \frac{\rho\cos\theta - x}{\sin\theta} = \frac{y - \rho\sin\theta}{\cos\theta} = y\cos\theta - x\sin\theta. \tag{4}$$

In order to apply the Radon transform on a 2-D digital image $g(m,n)$ of size MxN, we first sample continuous variables:

$$\begin{aligned}
&x = x_m = x_{\min} + m, && m = 0,1,...,M-1,\\
&y = y_n = y_{\min} + n, && n = 0,1,...,N-1,\\
&\theta = \theta_t = \theta_{\min} + t\cdot\Delta\theta, && t = 0,1,...,T-1,\\
&\rho = \rho_r = \rho_{\min} + r\cdot\Delta\rho, && r = 0,1,...,P_\theta - 1,\\
&s = s_k = s_{\min} + k\cdot\Delta s, && k = 0,1,...,S_{\rho,\theta} - 1,
\end{aligned} \tag{5}$$

where we set:

$$\begin{aligned}
&x_{\min} = -x_{\max} = -(M-1)/2, \quad && y_{\min} = -y_{\max} = -(M-1)/2,\\
&\rho_{\min} = -\rho_{\max} = -\frac{(P_\theta - 1)}{2}\Delta\rho, \quad && s_{\min} = -s_{\max} = -\frac{(S_{\rho,\theta} - 1)}{2}\Delta s.
\end{aligned} \tag{6}$$

Here, for simplicity and without loss of generality, we suppose that the image is square (i.e., M=N) and M is odd. Furthermore, if we consider $\theta_{\min}$=0, $\Delta\theta$ should be π/T to let θ span π. We also set $\Delta\rho$ and T to 1 and π, respectively.

The values of the remaining parameters Δs, P_θ, and $S_{\rho,\theta}$ are not fixed and depend on ρ and/or θ. They should be set precisely to let all pixels of the image be utilized in the Radon transform for any angle θ. Fig. 2 represents two examples of applying the Radon transform on an image of size 5x5 (i.e., M=5) for two different angles. Considering the examples, and using (4) and (5), Δs and P_θ can be suitably approximated as

$$\begin{aligned}
&\Delta s = \begin{cases} \dfrac{1}{|\cos\theta_t|}, & \sin\theta_t \le \sin\dfrac{\pi}{4} = \dfrac{1}{\sqrt{2}} \\ \dfrac{1}{\sin\theta_t}, & \sin\theta_t > \sin\dfrac{\pi}{4} = \dfrac{1}{\sqrt{2}} \end{cases}\\
&P_\theta \approx \lceil M\cdot\Delta s\rceil + 1 - (\lceil M\cdot\Delta s\rceil \bmod 2),
\end{aligned} \tag{7}$$

where $\lceil . \rceil$ represents the ceiling operation, and P_θ is adjusted to take an odd integer value.

The approximation of $S_{\rho,\theta}$, is rather complicated, since the value of $S_{\rho,\theta}$ depends on both ρ and θ. While it is fixed and equal to M for some values of ρ, it is arithmetically decreased in a series afterwards, depending on both ρ and θ. Here, we skip details which are not a matter of importance for our work.

$$S_{\rho,\theta} \approx \begin{cases} M, & |\rho_r| \le \rho_{const} \\ M - \lceil (|\rho_r| - \rho_{const})\cdot d \rceil, & |\rho_r| > \rho_{const} \end{cases}. \tag{8}$$

Further, ρ_{const} and d are:

$$\begin{aligned}
&\rho_{const} = \left\lfloor \frac{M-1}{2}\cdot\left| |\cos\theta_t| - \sin\theta_t \right| \right\rfloor,\\
&d = \frac{2(\alpha\cdot M - \beta)}{\alpha(\alpha - 1)},\\
&\alpha = \left(\frac{P_\theta - 1}{2}\right) - \rho_{const} + 1,\\
&\beta = \frac{M^2}{2} - M\cdot\rho_{const},
\end{aligned} \tag{9}$$

where [.] represents the rounding operation.

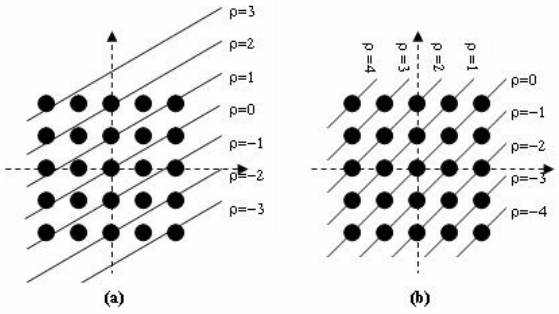

Figure 2. An example of applying Radon transform on an image with M=5. (a) reference lines for θ=120°, (b) reference lines for θ=135°.

In approximating $S_{\rho,\theta}$, we also assume that each pixel assigned to its nearest reference line. In other words, as it can be seen from Fig. 2, the pixels are not always exactly on the reference lines. Here, without loss of generality, we simply apply a rounding operation to find the best choice, instead of more complicated interpolation mechanisms that may be used now and then [2]. Basing on this fact, let define x'_k and y'_k as

$$\begin{aligned} x'_k &= \lfloor \rho_r \cdot \cos\theta_t - s_k \cdot \sin\theta_t - x_{\min} \rceil, \\ y'_k &= \lfloor \rho_r \cdot \sin\theta_t + s_k \cdot \cos\theta_t - y_{\min} \rceil. \end{aligned} \tag{10}$$

The discrete Radon transform of a 2-D digital image $g(m,n)$ is then approximated from (3) as

$$R(\rho_r,\theta_t) \approx \Delta s \cdot \sum_{k=0}^{S_{\rho,\theta}-1} g(x'_k, y'_k). \tag{11}$$

III. Proposed Approach

A. Motivation

As it was mentioned before, despite the capability of the Radon transform in line (-trend) detection in images, it suffers from two inherent problems that prevent the Radon transform to become a complete tool for rotation-invariant image analysis applications. The source of these problems arises from this fact that in the Radon transform, the number of pixels projected on a line is not necessarily the same for different directions and/or coordinates of a direction. This point can be recognized easily in Fig. 2 and also mathematically verified from (8), where it is seen that the number of pixels $S_{\rho,\theta}$ on the line along the s-axis depends on ρ and θ.

Consequently, the results of the Radon transform that is the summation of all coordinates along this line may not act in a similar statistical base for different parameters ρ and/or θ. In next sections, we propose two new transforms based on the definition of the discrete Radon transform in (11) to solve the abovementioned problems.

B. First Proposed Transform

Define a set $\Phi^{r,t}$ as

$$\Phi^{r,t} = \left\{ (x'_i, y'_i) : \rho = \rho_r \text{ and } \theta = \theta_t,\ i = 0,1,...,S_{\rho,\theta}-1 \right\}. \tag{12}$$

Using (12), equation (11) can be rewritten as

$$R(\rho_r,\theta_t) \approx \Delta s \cdot \sum_{k=0}^{S_{\rho,\theta}-1} \phi_k^{r,t}, \tag{13}$$

where $\phi_k^{r,t}$ is the k^{th} element of the set $\Phi^{r,t}$.

Furthermore in (13), we can substitute the summation with the sample mean operator as

$$R(\rho_r,\theta_t) \approx \Delta s \cdot S_{\rho,\theta} \cdot \text{Mean}(\Phi^{r,t}). \tag{14}$$

Using (14), we define the *first proposed transform* R_1 as

$$R_1(\rho_r,\theta_t) \equiv \Delta s \cdot \text{Mean}(\Phi^{r,t}). \tag{15}$$

Since the sets $\{\Phi^{r,t} \mid r=0,1,\ldots,P_\theta - 1 \text{ and } \theta=\theta_t\}$ have different number of elements, we can expect a more stabilized statistical behavior as compared to the conventional Radon transform, if we use sample mean as it is done in (15), instead of summation in (13). Thus, we can expect a better performance for direction estimation. This fact will be shown through experiments later.

Comparing (14) and (15), it can be easily seen that there is a linear relation between the conventional Radon transform and the one we defined here as the first proposed transform:

$$R(\rho_r,\theta_t) = \frac{1}{S_{\rho,\theta}} \cdot R_1(\rho_r,\theta_t). \tag{16}$$

So, R_1 inherits almost all properties of the Radon transform such as linearity, shifting, rotation and so on [2]. Also, we expect R_1 has approximately the same processing time as the Radon transform.

C. Second Proposed Transform

Using (8) and (9), it can be easily shown that the total number of elements for any arbitrary direction θ_t in the sets $\{\Phi^{r,t} \mid r=0,1,\ldots,P_\theta - 1 \text{ and } \theta=\theta_t\}$ is almost M^2, where M is the dimensions of a 2-D square image. In other words,

$$\sum_{r=1}^{P_\theta} S_{\rho,\theta} \approx M^2. \tag{17}$$

Now, we define Ψ^t as a set of successive concatenations of the sets $\{\Phi^{r,t} \mid r=0,1,\ldots,P_\theta - 1 \text{ and } \theta=\theta_t\}$:

$$\Psi^t = \text{Concat}(\Phi^{r,t}),\ r = 0,1,...,P_\theta - 1 \text{ and } \theta = \theta_t. \tag{18}$$

Using (18), the *second proposed transform* R_2 is then defined as

$$R_2(\lambda_j,\theta_t) \equiv \Delta s \cdot \text{Mean}(\Psi_j^t),\ j = 0,1...,M-1, \tag{19}$$

where Ψ_j^t is the j^{th} M-elements subset[1] of the set Ψ^t (Fig 3), and λ_j is defined as

$$\lambda = \lambda_j = \lambda_{\min} + j, \qquad j = 0,1,...,M-1. \tag{20}$$

As a result, R_2 has no longer a linear relation with the Radon transform, because we apply the mean operator on collections with the equal number of elements instead of the sets $\{\Phi^{r,t} \mid r=0,1,\ldots,P_\theta - 1 \text{ and } t=0,1,\ldots,T-1\}$ with the non-equal number of elements. The fact can be more clarified if we compare ρ_t and λ_j in Fig. 3.

[1] For a non-square image, Ψ_j^t is the j^{th} N-elements subset, where the size of the image is MxN, and for any arbitrary block of an image, Ψ_j^t is the j^{th} K-elements sunset, where the size of the block is MxK.

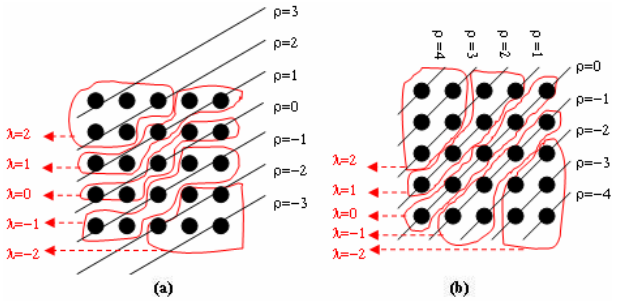

Figure 3. Applying the second proposed transform on examples of Fig. 2. The figures show how the sets Ψ_j^t with equal numbers of elements are extracted from the sets $\Phi^{r,t}$ with different numbers of elements for two different directions.

For the second proposed transform, we can expect a faster processing time compared to the Radon transform, because the matrix simplification techniques are widely applicable at time. We will also examine this fact later.

D. Applications in Direction Estimation

For image analysis applications, we usually need to extract some features from an image and then develop our approaches based on those features. Among the different features, texture is one of the most important ones, due to its presence in most real world images which makes it under high attention for many applications in content-based image representation and retrieval, medical imaging, remote sensing, and so on.

However, the problem with the majority of existing works on texture analysis is that it is assumed that all images are acquired from the same orientation. This assumption is not realistic in practical applications, where images may be taken with different rotation, scale, etc. As a result, the performance of these methods becomes worse when this underlying assumption is no longer valid.

There are many methods proposed to address the problem of the rotation-invariant texture analysis [8], where almost all of them try to estimate the directional information in an image. Among them, there are some works that utilize the Radon transform for this purpose [5],[6]. Here, we consider these approaches and show that the proposed transforms achieve this goal significantly better than the Radon transform.

Generally the texture of an image consists of anisotropic (directional) and/or isotropic (non-directional) textures [9]. In this respect, textures may be divided into four different categories: (i) anisotropic with one dominant direction; (ii) multidirectional anisotropic; (iii) isotropic; and (iv) mixed, where the dominant direction for a texture is defined as the direction with more straight lines.

Basing on this fact, we can estimate the directional information for an image with directional textures in their structures using the Radon transform. For this purpose, the Radon transform is usually calculated for all directions with θ_t from 0° to 179°. We then compute the variance of the result for each direction, and form the variance array S_R as

$$S_R(\theta) = Var_{\theta_t \in [0,180)}[R(\rho_r, \theta_t)]. \qquad (21)$$

Figs. 4-7 show the variance arrays for four images with different kinds of textural structure and their 30° rotated versions. For comparison, we depict the variance array for the Radon transform as well as the proposed transforms, where the variance arrays for the first and second transforms are calculated, substituting R by R_1 and R_2 in (21), respectively.

However, in the case of the conventional Radon transform, since it is not an isotropic method as mentioned before, we applied it on a disk shape area from the middle of images to get a better result.

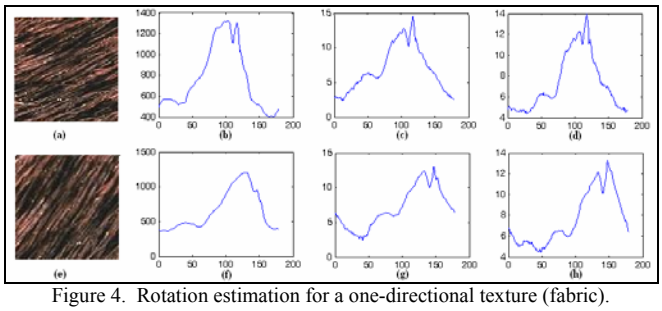

Figure 4. Rotation estimation for a one-directional texture (fabric).

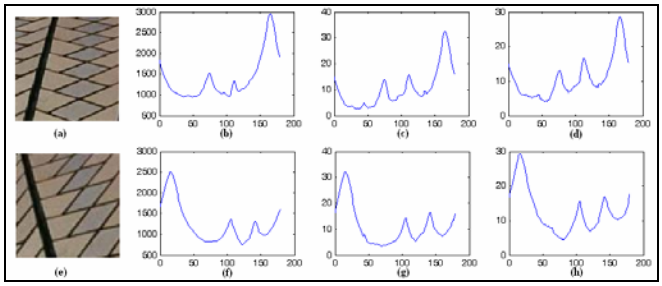

Figure 5. Rotation estimation for a multidirectional texture (tile).

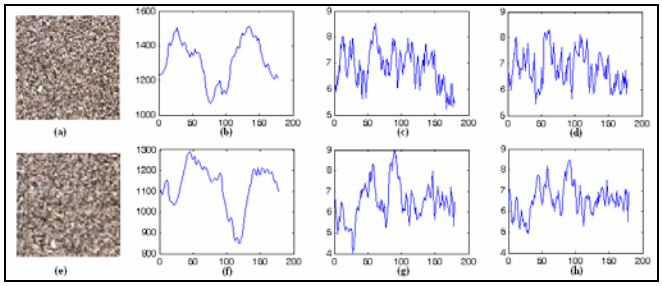

Figure 6. Rotation estimation for an isotropic texture (fabric).

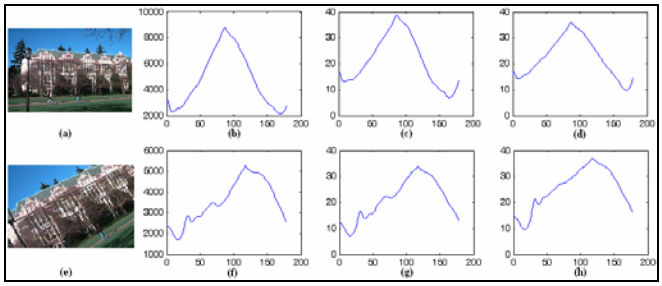

Figure 7. Rotation estimation for a mixed texture (a building, trees, and sky). (a) original image, (b) variance array of the original image, applying the Radon transform (c) variance array of the original image, applying the first proposed transform (d) variance array of the original image, applying the second proposed transform (e) a 30° rotated version of the image, (f) variance array of the rotated image, applying the Radon transform (g) variance array of the rotated image, applying the first proposed transform (h) variance array of the rotated image, applying the second proposed transform.

From Figs. 4-7, we can see that in the case of an anisotropic texture, the variance array has a large value in the direction perpendicular to the dominant direction. It means that the Radon transform (or any of the proposed ones) has larger variations along the dominant direction which is in an agreement with the definition of the Radon transform. In fact, a variance array is expected to have a global maximum at this direction for an anisotropic texture. Thus, the dominant direction D can be estimated as

$$D = \arg\max_{\theta_i}(S_R) - 90°. \quad (22)$$

Now, considering the global maxima of the variance arrays of the original images (D_0) and the rotated images (D_{30}) in Figs. 4-7, their differences are expected to be equal to the rotation angle 30°. From these figures it can be seen that for the proposed transforms, the differences are precisely or almost precisely equal to 30°, even in the case of an isotropic image whose spectrum does not change significantly by rotation [5]. However, for the Radon transform, this is not true and estimates are not as good as the proposed transforms.

IV. Experimental Results

In the first experiment, we evaluated the correct estimates of the dominant directions on a dataset with 4080 images that has been already used in [5]. For generating the dataset, we utilized 60 images of size 512x512 from the Brodatz album. Fig. 8 exhibits the images, including 8 one-directional textures D16, D49, D50, D51, D68, D76, D77, and D105; 13 (almost purely) isotropic textures D4, D5, D9, D23, D24, D27, D28, D48, D66, D74, D75, D98, and D110; and 17 mixed textures (including semi-isotropic textures) D8, D10, D11, D19, D25, D37, D46, D57, D81, D83, D84, D85, D86, D87, D92, D101, and D111. The remaining images are multidirectional textures.

Each image was then divided into 256x256 nonoverlapping blocks, and one 128x128 subimage was extracted from the middle of each block. In order to create rotated versions of these subimages, each 256x256 block was rotated at angles 10° to 160° with step size 10° and then from each rotated block, one 128x128 subimage was selected from its middle.

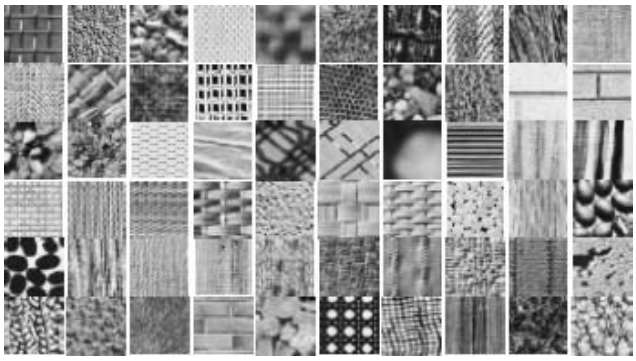

Fig. 8. 60 typical images from the Brodatz album. From left to right:
1st row: D1, D4, D5, D6, D08, D9, D10, D11, D15, D16.
2nd row: D17, D18, D19, D20, D21, D22, D23, D24, D25, D26.
3rd row: D27, D28, D34, D37, D46, D47, D48, D49, D50, D51.
4th row: D52, D53, D55, D56, D57, D64, D65, D66, D68, D74.
5th row: D75, D76, D77, D78, D81, D82, D83, D84, D85, D86.
6th row: D87, D92, D93, D94, D98, D101, D103, D105, D110, D111.

Keeping non-rotated images as references for comparison, the dominant direction was then estimated for other 3840 images based on the procedure described in Section III.D. Here, the estimation is supposed to be correct if the following condition is satisfied:

$$\left|\alpha_R - \left(D_0 - D_{\alpha_R}\right)\right| \le \text{deviation}, \quad (23)$$

where α_R is the rotation angle, and D_0 and $D\alpha_R$ are the dominant directions of the non-rotated and rotated images, respectively, calculated using (22).

TABLE I. Correct Detection Rate in Different Transforms for Images with One-Directional Textural Structures

Texture Category (deviation)	Correct Detection Rate		
	Radon Transform	*Proposed Transform I*	*Proposed Transform II*
One-Directional (deviation<=1)	71.5%	95.3%	94.5%
One-Directional (deviation<=3)	75.4%	98.2%	98.6%
One-Directional (deviation<=5)	77.1%	99.2%	99.0%

TABLE II. Correct Detection Rate in Different Transforms for Images with Multi-Directional Textural Structures

Texture Category (deviation)	Correct Detection Rate		
	Radon Transform	*Proposed Transform I*	*Proposed Transform II*
Multi-Directional (deviation<=1)	55.0%	85.4%	86.8%
Multi-Directional (deviation<=3)	64.9%	89.8%	89.9%
Multi-Directional (deviation<=5)	74.5%	90.3%	91.3%

TABLE III. Correct Detection Rate in Different Transforms for Images with Mixed Textural Structures

Texture Category (deviation)	Correct Detection Rate		
	Radon Transform	*Proposed Transform I*	*Proposed Transform II*
Mixed (deviation<=1)	51.5%	69.3%	66.9%
Mixed (deviation<=3)	58.7%	76.2%	74.6%
Mixed (deviation<=5)	66.7%	80.6%	80.1%

TABLE IV. Correct Detection Rate in Different Transforms for Images with Isotropic Textural Structures

Texture Category (deviation)	Correct Detection Rate		
	Radon Transform	*Proposed Transform I*	*Proposed Transform II*
Isotropic (deviation<=1)	41.3%	54.5%	55.4%
Isotropic (deviation<=3)	50.7%	63.2%	65.0%
Isotropic (deviation<=5)	56.4%	68.6%	71.4%

The results of the correct detection rate for each category have been summarized in Tables I to IV for different values of deviation. As expected, the results proved that both proposed transforms outperform the Radon transform significantly, for all kinds of images with different textural categories.

For the second experiment, we examined the performance of the transforms in the presence of the additive noise to evaluate their robustness to noise. For this purpose, we highly distorted images by adding Gaussian random noises with zero means and SNR=0db. Results for deviation=3 in (23) are shown in Table V. Comparing Table V with Tables I-IV, we see that the transforms are highly robust to the noise.

TABLE V.ROBUSTNESS TO NOISE FOR DIFFERENT TRANSFORMS

Texture Category (deviation=3)	**Correct Detection Rate**		
	Radon Transform	***Proposed Transform I***	***Proposed Transform II***
One-Directional	72.9%	96.5%	96.9%
Multi-Directional	64.1%	87.6%	87.6%
Mixed	57.7%	73.8%	72.2%

Finally, in the last experiment, we computed the processing time needed to perform each transform. Table VI shows the results in millisecond for an image of size 128x128 on a work station computer with CPU 3.06 GHz and 2GB RAM. Results indicate that the second proposed transform is considerably faster than the conventional and the first proposed ones.

TABLE VI.PROCESSING TIME FOR DIFFERENT TRANSFORMS

	Radon Transform	***Proposed Transform I***	***Proposed Transform II***
Processing Time	482ms	543ms	159ms

V. CONCLUSIONS AND FUTURE WORKS

In this paper, we proposed two new transforms based on the Radon transform which is a well-developed tool in the field of image analysis. Through the paper, we discussed that while the proposed transforms preserved the most important characteristics of the conventional discrete Radon transform, they solved the inherent problems of the Radon transform in detecting the directional information of an image.

Experimental results indicated a considerable increase in the performance of the direction estimation in images using the proposed transforms compared to the Radon transform. Experiments also showed that the processing time for the second proposed transform (19) was significantly faster. This property makes this transform very interesting for applications such as content-based image retrieval whose reply times should be as short as possible.

In future, we plan to extend the idea to the continuous domain as well as to generalize the definition of the proposed transforms for any kinds of curves rather than straight lines. The applicability of the transforms to other domains such as content-based image retrieval (CBIR) will be also studied and examined in later works.

ACKNOWLEDGMENT

This work was supported in part by the Institute for Information Technology Advancement (IITA) and in part by the Korean Ministry of Information and Communication (MIC) through the Realistic Broadcasting Research Center (RBRC) at Gwangju Institute of Science and Technology (GIST).

REFERENCES

[1] S.R. Deans, "The radon transform and some of its applications," Eds. John Wiley and Sons: New York, 1983.

[2] P. Toft, "Radon transform: theory and implementation," PhD Thesis, IMM, DTU, 1996.

[3] E. Magli, L. Lo Presti, and G. Olmo, "A pattern detection and compression algorithm based on the joint wavelet and Radon transform," in Proc. of IEEE 13th Int. Conf. Digital Signal Processing, vol. 2, pp. 559-562, Jul 1997.

[4] A.L. Warrick and P.A. Delaney, "Detection of linear features using a localized Radon transform with a wavelet filter," in Proc. of ICASSP, vol. 4, pp. 2769-2772, Apr 1997.

[5] K.Jafari-Khouzani and H.Soltanianzadeh, "Radon transform orientation estimation for rotation invariant texture Analysis," IEEE Trans. on Pattern Analysis and Machine Intelligence, vol. 27 (6), pp.1004-1008, Jun 2005.

[6] M.R. Hejazi, Y.S. Ho, "A hierarchical approach to rotation-invariant texture feature extraction based on Radon transform parameters," in Proc. of IEEE ICIP2006, in press.

[7] P. Brodatz, "Texture: a photographic album for artists and designers," New York, 1966.

[8] J. Zhang and T. Tan, "Brief review of invariant texture analysis methods," Pattern Recognition, vol. 35, pp. 735-747, Mar 2002.

[9] K.J. Dana, B.V. Ginneken, S.K. Navar, and J.J. Koenderink, "Reflectance and texture of real-world surfaces," ACM Trans. on Graphics, Vol. 18 (1), pp. 1-34, Jan 1999.